

# Synthesis, Reactivity, and Bonding Analysis of a Tetracoordinated Nickel Carbene

Pablo M. Pérez-García,<sup>1,2‡</sup> María L. G. Sansores-Paredes,<sup>1‡</sup> Célia Fonseca Guerra,<sup>3</sup> Pascal Vermeeren,<sup>3\*</sup> and Marc-Etienne Moret<sup>1\*</sup>

<sup>1</sup> Organic Chemistry and Catalysis, Institute for Sustainable and Circular Chemistry, Faculty of Science, Utrecht University, Universiteitsweg 99, 3584 CG, Utrecht, The Netherlands.

<sup>2</sup> Universidad Privada Boliviana (UPB), Cochabamba, Bolivia

<sup>3</sup> Department of Chemistry and Pharmaceutical Sciences, AIMMS, Vrije Universiteit Amsterdam, De Boelelaan 1108, 1081 HZ Amsterdam, The Netherlands.

**ABSTRACT:** Nickel carbenes are key reactive intermediates in the catalytic cyclopropanation of olefins and other reactions, but isolated examples are scarce and generally rely on low coordination numbers ( $\leq 3$ ) to stabilize the metal–ligand multiple bond. Here we report the isolation and characterization of a stable tetracoordinated nickel carbene bearing a triphosphine pincer ligand. Its nucleophilic character is evidenced by reaction with acids, and it can transfer the carbene fragment to CO to form a ketene. A computational study of the Ni=C bond sheds light on the role of the third phosphine in the pincer framework to the stabilization of the nickel carbene fragment.

Metal carbenes are important intermediates for many broadly applied chemical reactions such as cyclopropanations,<sup>1</sup> cross-couplings,<sup>2</sup> and olefin metathesis.<sup>3</sup> A detailed understanding of the reactivity of these organometallic entities is necessary to fully exploit their catalytic potential, both to optimize known reactions and to develop new ones. First row transition metal centers are of high current interest, because of not only their earth-abundance but also their high reactivity.<sup>4,5</sup>

Early work by Miyashita and Grubbs<sup>6,7</sup> suggested the potential of nickel carbenes generated by the fragmentation of metallacycles for olefin metathesis and cyclopropanation. However, the stabilization of such species is challenging because of the electron rich nature of nickel and the strong  $\sigma$ -donation of the carbene fragment. Several years later, based on the conceptualization that a " $L_2Ni$ " moiety has isolobal orbitals with the  $CH_2$  fragment, the group of Hillhouse pioneered the synthetic study of nickel carbene species.<sup>8,9</sup> They described the isolation and thorough characterization of nickel carbene complexes bearing the dtbpe ligand (bis(di-tert-butylphosphino)ethane = dtbpe) and another related rigid bidentate ligand (Figure 1). To the best of our knowledge these are the only examples of isolated nickel carbenes that are neither heteroatom-stabilized (e.g., NHCs)<sup>10</sup> nor incorporated in a multidentate (e.g., pincer) ligand.<sup>11</sup>

The dtbpe-supported nickel carbene complex undergoes nucleophilic addition to two molecules of  $CO_2$  to form an 1,1-dicarboxylate ligand, and it can transfer the carbene fragment to small molecules such as CO and ethylene to form the corresponding ketene and cyclopropane, respectively.<sup>8</sup> In the case of the reaction with ethylene, a metallacyclobutane intermediate was proposed.<sup>12</sup>

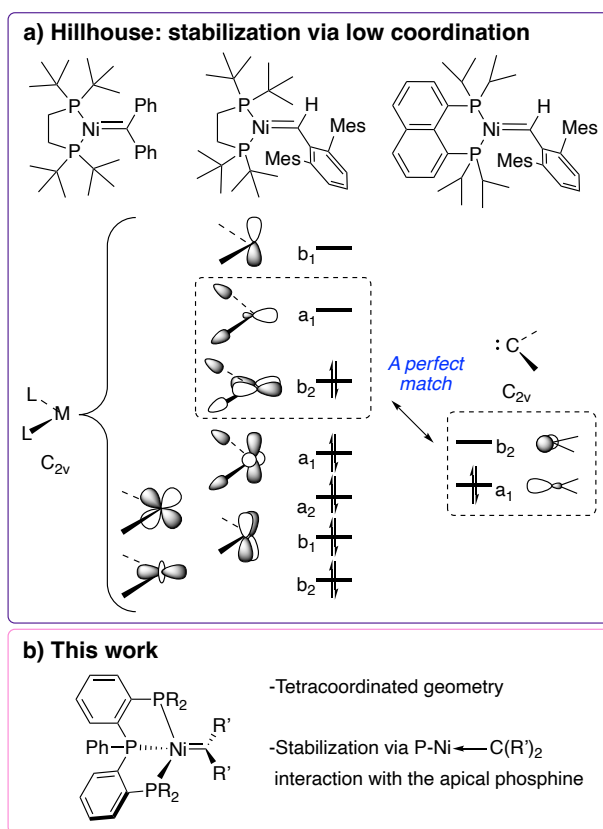


**Figure 1.** a) Nickel carbenes reported by Hillhouse,<sup>8,9,13</sup> b) tetracoordinated nickel carbene presented in this work.

Our group recently investigated the reactivity of pentacoordinated nickelacyclobutanes with distorted trigonal bipyramidal geometry incorporated in a pincer framework.<sup>14</sup> In agreement with the early observation from Miyashita that the metathesis-

like fragmentation of nickelacyclobutanes could be favored by higher coordination numbers,<sup>15</sup> selective [2+2] cycloreversion could be observed in one case. This contrasts with the known reactivity of square planar nickelacyclobutanes, for which no metathesis-like fragmentation has been observed. For a putative olefin-metathesis cycle based on a 5-coordinate nickelacyclobutane to be viable, the corresponding 4-coordinate Ni carbene would also need to be stable despite deviating from the isolobal paradigm outlined above.

In this work, we investigate whether such a species can be supported by a tridentate phosphine ligand. We present the synthesis of a well-defined tetracoordinated nickel carbene complex bearing a triphosphine pincer ligand and study its reactivity. DFT calculations<sup>16-18</sup> and Energy Decomposition Analyses (EDA) within the framework of quantitative Kohn-Sham molecular orbital theory<sup>19-22</sup> are used to shine light onto the bonding situation of the tetracoordinated nickel carbene.

Reduction of the previously reported  $\text{PPP}^{p\text{-tol}}\text{Ni}^{\text{I}}\text{Br}$  complex<sup>23</sup> with sodium naphthalenide afforded well-defined Ni(0) complex **1** bearing only nitrogen as coligand (Figure 2 and Figures S1-S5). Treating complex **1** with 1 equivalent of  $\text{N}_2\text{C}(p\text{-anisyl})_2$  resulted in instantaneous complete conversion to two new species detected by  $^{31}\text{P}\{^1\text{H}\}$  NMR analysis (Figure S6). The IR spectrum of the reaction mixture showed a strong signal at  $2030\text{ cm}^{-1}$ , supporting the presence of a Ni(0) diazo complex as major species (Figure S7), which is associated with broad  $^{31}\text{P}$  NMR signals at 20 and 75 ppm. This species cleanly converted into the initially minor product **2** over five days at room temperature. The latter displayed a clear triplet and doublet at 57.9 and 47.6 ppm in  $^{31}\text{P}$  NMR (Figure 2). Gratifyingly,  $^{13}\text{C}\{^1\text{H}\}$  NMR analysis revealed that compound **2** is a Ni-carbene complex with a diagnostic signal at 288.8 ppm (Figure 2 and S10). The doublet of triplet multiplicity (dt,  $^2J_{\text{C,P}} = 30\text{ Hz}$ ,  $^2J_{\text{C,P}} = 17\text{ Hz}$ ) confirms that all three phosphine moieties are bound to Ni. The assignment is additionally confirmed by the observation of three-bond  $^1\text{H}\text{-}^{13}\text{C}$  coupling by HMBC analysis (Figure S13). Complex **2** was isolated in 61 % yield as a black solid.

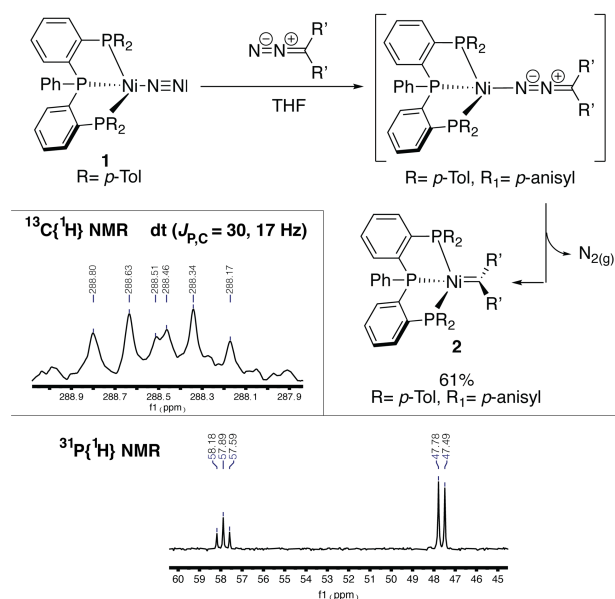
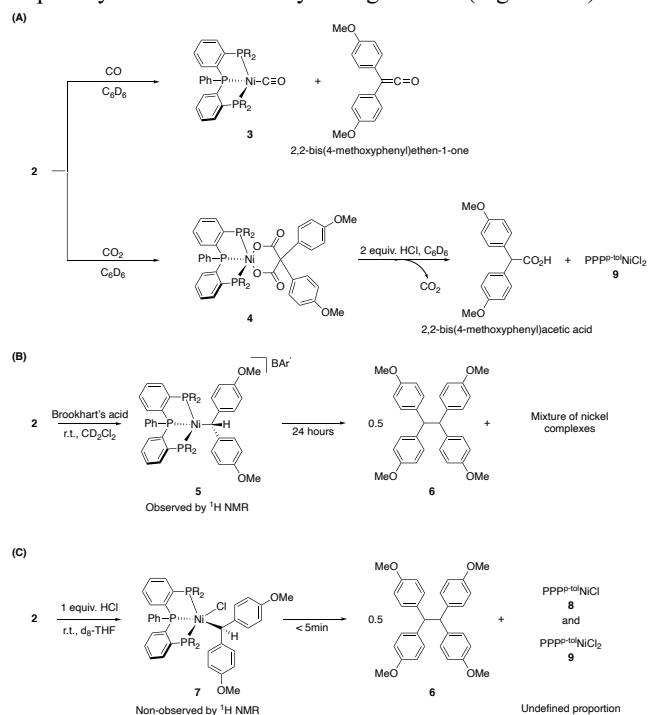


**Figure 2.** Synthesis of nickel carbene **2** bearing pincer ligand  $\text{PPP}^{p\text{-tol}}$  and relevant NMR spectra.

Complex **2** reacts rapidly with CO (1 atm) in  $\text{C}_6\text{D}_6$ , showing a solution color change from black to light yellow (Scheme 1, A). NMR and IR analysis show the total conversion of complex **2** to free 2,2-bis(4-methoxyphenyl)ethen-1-one and complex  $(\text{PPP}^{p\text{-tol}}\text{Ni}^0(\text{CO}))$  (**3**, Figures S16 and S18), which could also be independently generated from complex **1** with CO (Figures S14 and S15). This result demonstrates the ability of **2** to transfer the carbene fragment to a small molecule in milder conditions than reported for  $(\text{dtbpe})\text{NiCPh}_2$ . The reaction of complex **2** with  $\text{CO}_2$  led to the formation of a metallalactone complex **4** via a possible [2+2] sequential cycloaddition of two  $\text{CO}_2$  equivalents (Figures S19-S21). Strong IR ester signals at  $1602\text{ cm}^{-1}$  and  $1643\text{ cm}^{-1}$ , similar to those reported by Hillhouse,<sup>8</sup> testify the presence of two ester groups in the metallacycle. In addition, the reaction complex **4** with HCl in ether leads to the formation of 2,2-bis(4-methoxyphenyl)acetic acid, the expected product of protolysis of the dicarboxylate ligand in **4** (Figure S24).<sup>24</sup>



**Scheme 1.** (A) Reactivity of complex **2** with CO and  $\text{CO}_2$ . (B) Reaction of complex **2** with Brookhart's acid (C) Reaction of complex **2** with HCl.

As nickel carbenes are generally nucleophilic,<sup>25</sup> we also investigated the protonation of compound **2**. The reaction with Brookhart's acid  $[\text{H}(\text{OEt}_2)_2]^+[\text{3,5-(CF}_3)_2\text{C}_6\text{H}_3]_4\text{B}^-$  in  $\text{CD}_2\text{Cl}_2$  at room temperature (Scheme 1, B) was first tested. A  $^1\text{H}$  multiplet centered at 4.93 ppm, shown to couple to three  $^{31}\text{P}$  nuclei by  $^1\text{H}\{^{31}\text{P}\}$  NMR analysis, suggests the formation of transient  $\text{Ni}^{\text{II}}(\text{alkyl})$  complex **5** in the reaction mixture. Over time, complex **5** degrades to form coupling product **6** (1,1,2,2-tetrakis(4-methoxyphenyl)ethane) and a complex mixture of Ni complexes (Figures S27 and S28). In contrast, the reaction of **2** with one equivalent of HCl (diethyl ether solution, Scheme 1, C) in  $\text{d}_8\text{-THF}$  at room temperature led to the rapid formation of a stoichiometric amount of **6** together with a mixture of paramagnetic complex  $(\text{PPP}^{p\text{-tol}}\text{Ni}(\text{Cl}))$  (**8**) and diamagnetic complex  $(\text{PPP}^{p\text{-tol}}\text{NiCl}_2)$  (**9**). EPR analysis confirmed the presence of complex **8**, and  $^{31}\text{P}\{^1\text{H}\}$  NMR analysis confirmed the presence of complex **9** (Figures S31 and S32). To account for these observations, we propose the initial formation of a  $\text{Ni}^{\text{II}}(\text{alkyl})$  complex

(either 5 or 7), which undergoes homolytic cleavage of the nickel alkyl ligand bond (Scheme 1B and 1C) to form a Ni<sup>I</sup> center and a stabilized alkyl radical that ultimately dimerizes to form 6. This contrasts with the reactivity of the dtbpe analogue, for which the Ni<sup>II</sup>(alkyl) complex resulting from protonation is stable and can be isolated.<sup>8</sup>

DFT calculations<sup>16–18</sup> provide more insight into the nature of the nickel-carbene interaction in compound 2. First, the geometry of a slightly truncated model of 2 bearing phenyl instead of *p*-tolyl and *p*-anisyl substituents is optimized at M06L-D3/6-31g(d,p) (Figure 3). The nickel carbene 2 presents a distorted tetrahedral geometry where the calculated Ni–C bond length is somewhat longer (1.854 Å, Table 1) than the analogous bond of the optimized (dtbpe)NiCPh<sub>2</sub> (1.805 Å, Figure S32) and the corresponding X-ray crystal structure (1.836 (2) Å).<sup>8</sup> A conformational search reveals alternative geometries, involving the coordination of only two of the three phosphine moieties of the ligand, which are significantly less stable (Figure S33).

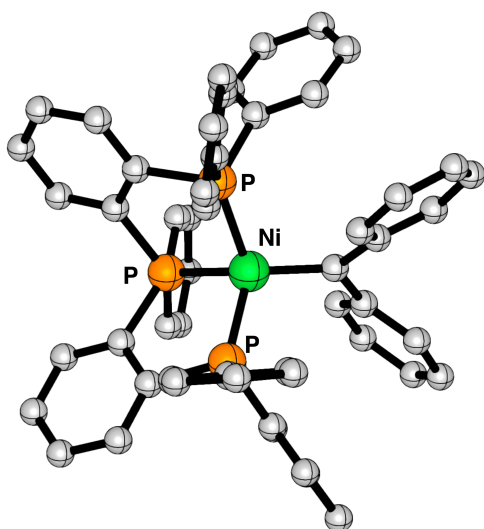


**Figure 3.** Optimized structure of 2 calculated at the M06L-D3/6-31g(d,p) level of theory. Hydrogens atom are omitted for clarity.

To get more insight into the chemical bonding of (PPP<sup>Ph</sup>)NiCPh<sub>2</sub>, Quantum Theory of Atoms in Molecules (QTAIM)<sup>26</sup> and Energy Decomposition Analyses (EDA) within the framework of quantitative Kohn-Sham molecular orbital theory<sup>19–22</sup> are performed. QTAIM is a topological analysis of the electron density that can provide information about the nature of the Ni–carbene bond as donor–acceptor interaction (Fischer carbenes, prone to nucleophilic attack at carbon) or covalent delocalized bonds (Schrock carbenes, carbon nucleophiles).<sup>27,28</sup> Analysis of the Laplacian map of the  $\pi$ -plane at the carbene carbon (perpendicular to the CPh<sub>2</sub> plane) of (PPP<sup>Ph</sup>)NiCPh<sub>2</sub> shows an area of charge depletion in the direction of the  $p_{\pi}$  orbital of the carbon atom of the carbene. This indicates that the electrons of the carbene fragment are primarily located in the  $sp^2$ -hybridized orbital, engaging in a donor–acceptor interaction with nickel, and the  $p_{\pi}$ -like orbital is depleted (Figure S34). Notably, the same feature is also observed for (dtbpe)NiCPh<sub>2</sub> (Figure S35). In contrast, analysis of the Laplacian map of the  $\pi$ -plane of Piers’ carbene pincer complex (PC<sub>carbene</sub>P)NiPPH<sub>3</sub> shows a charge concentration around the

carbon atom showing a delocalized Ni–C bonding reminiscent of Schrock carbenes (Figure S36).<sup>11,27</sup> These results suggest that, even though Ni carbenes exhibit nucleophilic reactivity (see above), their electronic structure can resemble that of a Fischer carbene. Similarly, Grubbs’ Ru-carbene catalysts have been shown to present characteristics of both Fischer and Schrock carbenes.<sup>29</sup>

The EDA is used to analyze and compare the bonding mechanism between the Ligand–Ni and the CPh<sub>2</sub> fragments in the Ni–carbene complexes (dtbpe)NiCPh<sub>2</sub> and (PPP<sup>Ph</sup>)NiCPh<sub>2</sub> (Table 1).<sup>16, 27, 30–31</sup> In this method, the interaction energy ( $\Delta E_{\text{int}}$ ) is decomposed into four physically meaningful terms: the classical electrostatic interaction ( $\Delta V_{\text{elstat}}$ ), the steric (Pauli) repulsion ( $\Delta E_{\text{Pauli}}$ ) arising from the repulsion between occupied closed-shell orbitals of both fragments, the orbital interaction ( $\Delta E_{\text{oi}}$ ) that accounts for donor–acceptor interaction between the fragments and polarization within a fragment, and the dispersion energy ( $\Delta E_{\text{disp}}$ ).<sup>19–22</sup> The EDA results reveal that the Ni–carbene bond is for our newly synthesized (PPP<sup>Ph</sup>)NiCPh<sub>2</sub> less stabilizing than for (dtbpe)NiCPh<sub>2</sub>, that is, the interaction energy is  $-83.9 \text{ kcal mol}^{-1}$  for (PPP<sup>Ph</sup>)NiCPh<sub>2</sub> and  $-98.6 \text{ kcal mol}^{-1}$  for (dtbpe)NiCPh<sub>2</sub>. This difference in interaction energy originates from (i) a more destabilizing steric (Pauli) repulsion; and (ii) less stabilizing orbital interactions for (PPP<sup>Ph</sup>)NiCPh<sub>2</sub> compared to (dtbpe)NiCPh<sub>2</sub>. The former is a direct consequence of the increased steric repulsion between the phenyl groups of (PPP<sup>Ph</sup>)Ni and CPh<sub>2</sub>, which are, due to their spatial orientation, in closer proximity than the *tert*-butyl groups of (dtbpe)Ni and CPh<sub>2</sub>. This, in fact, not only amplifies the steric (Pauli) repulsion but also forces the Ni–carbene bond length to be longer for (PPP<sup>Ph</sup>)NiCPh<sub>2</sub> (1.854 Å) compared to (dtbpe)NiCPh<sub>2</sub> (1.805 Å).

The reduction of stabilizing orbital interactions from  $-112.3 \text{ kcal mol}^{-1}$  for (dtbpe)NiCPh<sub>2</sub> to  $-94.2 \text{ kcal mol}^{-1}$  for (PPP<sup>Ph</sup>)NiCPh<sub>2</sub> can be directly understood by analyzing the molecular orbitals responsible for the interaction between the Ligand–Ni and the CPh<sub>2</sub> fragments in the Ni–carbene complexes, that is, (i)  $\sigma$ -bonding between the occupied  $sp^2$ -hybridized orbital of CPh<sub>2</sub> (HOMO<sub>CPh<sub>2</sub></sub>) and the unoccupied  $a_1$ -like orbital of Ligand–Ni (LUMO<sub>L–Ni</sub>); (ii)  $\pi$ -backbonding between the unoccupied  $p_{\pi}$ -like orbital of CPh<sub>2</sub> (LUMO<sub>CPh<sub>2</sub></sub>) and the occupied  $b_2$ -like orbital of Ligand–Ni (HOMO<sub>L–Ni</sub>) (Figure 4). As proposed by Hillhouse and coworkers,<sup>8</sup> the orbitals of the L<sub>2</sub>Ni fragment are a perfect match for both  $\sigma$ -bonding and  $\pi$ -backbonding interactions with the CPh<sub>2</sub> fragment (Figure 1). The perpendicular conformation of the carbene fragment in (dtbpe)NiCPh<sub>2</sub> stand to maximize the  $\pi$ -backbonding interaction. In the case of (PPP<sup>Ph</sup>)NiCPh<sub>2</sub>, however, both the HOMO and LUMO, engaging in the  $\sigma$ -bonding and  $\pi$ -backbonding interactions with the CPh<sub>2</sub>, are delocalized over the pincer ligand, which suppresses stabilizing orbital interactions. Kohn-Sham molecular orbital analysis quantifies this and demonstrates that both the  $\sigma$ -bonding and  $\pi$ -backbonding orbital interaction weaken from (PPP<sup>Ph</sup>)NiCPh<sub>2</sub> to (dtbpe)NiCPh<sub>2</sub>, due to a loss of build-up in stabilizing orbital overlap as a result of both a smaller HOMO<sub>L–Ni</sub> and LUMO<sub>L–Ni</sub> lobe at the external face of (PPP<sup>Ph</sup>)Ni and a longer Ni–carbene bond length (Figure S37). This further explains the facile reactivity of (PPP<sup>Ph</sup>)NiCPh<sub>2</sub> with small molecules like CO.<sup>8</sup>

**Table 1.** Energy decomposition analyses (in kcal mol<sup>-1</sup>) of the Ni–carbene complexes and Ni–carbene bond length (in Å).<sup>[a]</sup>

Complex	$\Delta E_{\text{int}}$	$\Delta V_{\text{elstat}}$	$\Delta E_{\text{Pauli}}$	$\Delta E_{\text{oi}}$	$\Delta E_{\text{disp}}$	$r(\text{Ni}\cdots\text{C})$
(dtbpe)NiCPh <sub>2</sub>	-98.6	-169.1	207.5	-112.3	-24.7	1.805
(PPP <sup>Ph</sup> )NiCPh <sub>2</sub>	-83.9	-176.0	223.9	-94.2	-37.6	1.854

[a] Computed at ZORA-BLYP-D3(BJ)/TZ2P//M06L-D3/6-31g(d,p).

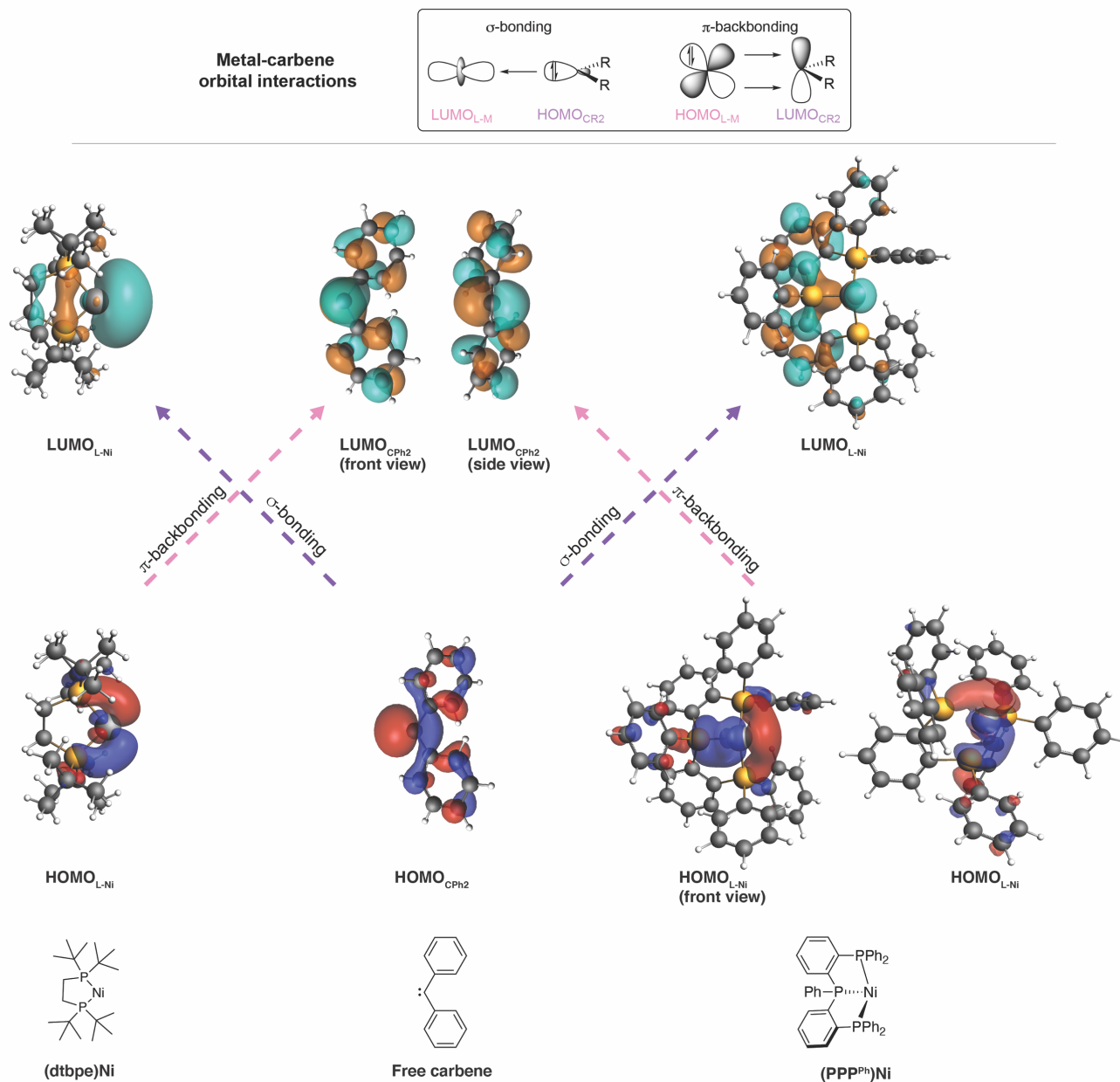


**Figure 4.** Molecular orbitals of the Ligand-Ni and carbene engaging in the  $\sigma$ -bonding (HOMO<sub>CPh<sub>2</sub></sub>–LUMO<sub>L-Ni</sub>) and  $\pi$ -backbonding (HOMO<sub>CPh<sub>2</sub></sub>–LUMO<sub>L-Ni</sub>) interaction, computed at ZORA-BLYP-D3(BJ)/TZ2P//M06L-D3/6-31g(d,p) level of theory.

Next, we aim to further study the influence of the phosphine ligand in apical position of (PPP<sup>Ph</sup>)NiCPh<sub>2</sub> on the Ni–carbene bond. To obtain a more detailed insight, we perform an EDA on simplified Ni–carbene complexes (Figure 5, see SI), where the phenyl groups bound to the phosphine ligands are replaced by hydrogen atoms and systematically go, in two steps, from the simplified (dtbpe)NiCPh<sub>2</sub> (complex A) to the simplified

(PPP<sup>Ph</sup>)NiCPh<sub>2</sub> without the apical phosphine ligand (complex B) to the simplified (PPP<sup>Ph</sup>)NiCPh<sub>2</sub> with the apical phosphine ligand (complex C). Our analyses reveal that the apical phosphine ligand polarized the occupied orbital density away from the external face, thereby reducing the steric (Pauli) repulsion between the simplified (PPP<sup>Ph</sup>)Ni and CPh<sub>2</sub> fragments and increasing the Ni–carbene bond strength. By going from

complex **A** to complex **B**, that is, by increasing the Ni–carbene bond length and P<sup>1</sup>–Ni–P<sup>2</sup> bond angle to that of (PPP<sup>Ph</sup>)NiCPh<sub>2</sub>, significantly weakens the Ni–carbene interaction from –87.7 kcal mol<sup>–1</sup> for **A** to –62.1 kcal mol<sup>–1</sup> for **B**. This weakening is a direct result of the increased steric repulsion between the phosphine ligands and CPh<sub>2</sub>, which are in closer proximity, as also reflected by the increase in steric (Pauli) repulsion. Introducing the apical phosphine ligand, hence having a complex that resembles (PPP<sup>Ph</sup>)NiCPh<sub>2</sub>, leads to a remarkable stabilization of the interaction energy from –62.1 kcal mol<sup>–1</sup> for **B** to –71.8 kcal mol<sup>–1</sup> for **C**. This

stabilization can be traced back to the π-accepting character of the apical phosphine ligand, which, upon binding, pulls occupied orbital density away from the incoming CPh<sub>2</sub> fragment, thereby lowering the destabilizing steric (Pauli) repulsion between the simplified (PPP<sup>Ph</sup>)Ni and CPh<sub>2</sub> fragments (Figure S41). This effect compensates the observed weakening of the stabilizing electrostatic and orbital interactions, corresponding to going from complex **B** to complex **C**.

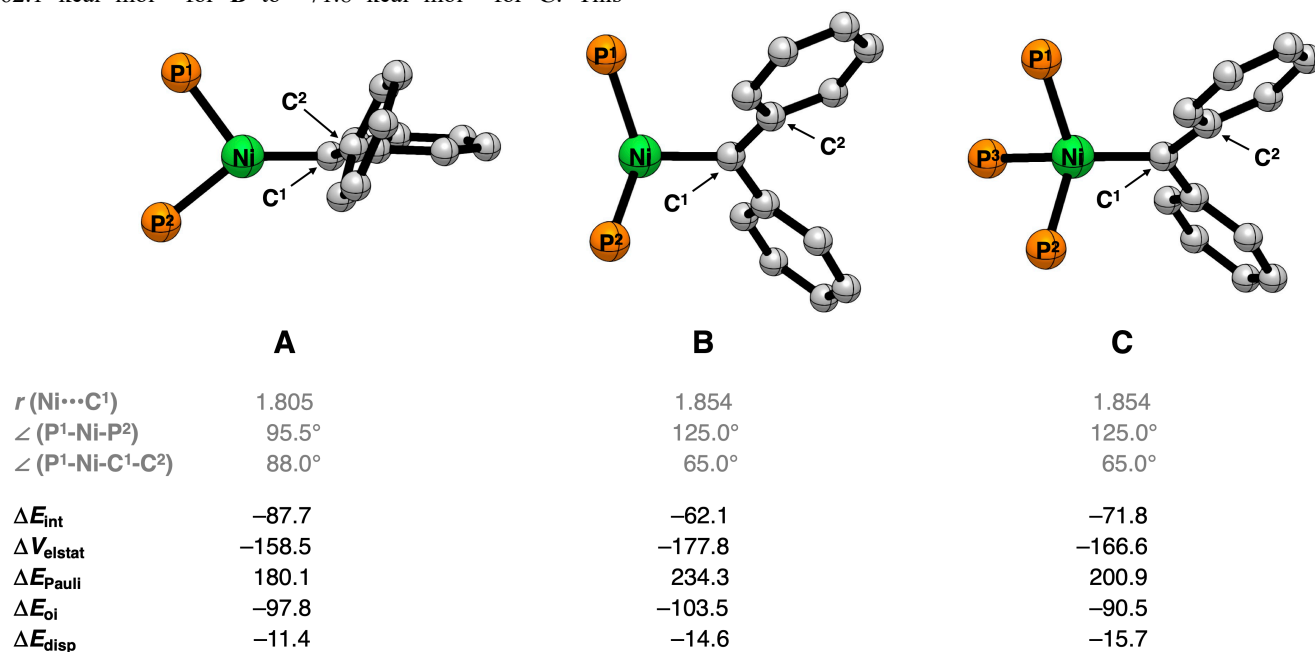


**Figure 5.** Energy decomposition analyses (in kcal mol<sup>–1</sup>) and geometrical parameters (in Å and °) of the simplified (PH<sub>3</sub>)<sub>2</sub>NiCPh<sub>2</sub> (**A**, **B**) and (PH<sub>3</sub>)<sub>3</sub>NiCPh<sub>2</sub> (**C**) complexes computed at ZORA-BLYP-D3(BJ)/TZ2P//M06L-D3/6-31(d,p) level. The simplified Ni–carbene complexes were constructed by replacing the phenyl substituents by hydrogen atoms from the optimized structures of (dtbpe)NiCPh<sub>2</sub> (complex **A**), (PPP<sup>Ph</sup>)NiCPh<sub>2</sub> without the apical phosphine ligand (complex **B**), and (PPP<sup>Ph</sup>)NiCPh<sub>2</sub> with the apical phosphine ligand (complex **C**). Hydrogens atom are omitted for clarity.

In conclusion, we report the synthesis and characterization of a stable tetracoordinated nickel carbene (PPP<sup>Ph</sup>-<sup>tol</sup>)NiC(*p*-anilyl)<sub>2</sub>. The complex is reactive towards small molecules such as CO and CO<sub>2</sub>, and its nucleophilic character is evidenced by its reactivity towards acids. Computational methods support the tetracoordinated geometry of (PPP<sup>Ph</sup>)NiCPh<sub>2</sub> as the most stable structure, with the Ni–C bond best viewed as a donor–acceptor interaction. EDA provides a view of the interaction between (PPP<sup>Ph</sup>)Ni and CPh<sub>2</sub> in this complex. This analysis shows that the key σ-bonding and π-backbonding interactions are possible for (PPP<sup>Ph</sup>)NiCPh<sub>2</sub> but somewhat weaker than for its 3-coordinate analogues. Interestingly, EDA also reveals that the third, apical phosphine ligand provides stabilization to the tetracoordinated nickel carbene by polarizing occupied orbital density away from its external face and thereby reducing the steric (Pauli) repulsion between (PPP<sup>Ph</sup>)Ni and CPh<sub>2</sub>. Overall, these results show that electron-rich metal carbenes can be stabilized even with relatively high coordination numbers, opening new possibilities for developing the chemistry of these reactive intermediates.

## ASSOCIATED CONTENT

Supporting Information.

Experimental section, spectra of new compounds and supplementary information of computational methods (pdf).

Cartesian coordinates of optimized structures (xyz).

This material is available free of charge via the Internet at <http://pubs.acs.org>.

## AUTHOR INFORMATION

### Corresponding Authors

\*Dr. Marc-Etienne Moret

Organic Chemistry and Catalysis

Institute for Sustainable and Circular Chemistry, Faculty of Science, Utrecht University, Universiteitsweg 99, 3584 CG, Utrecht, The Netherlands.

Email: [m.moret@uu.nl](mailto:m.moret@uu.nl)

\*Dr. Pascal Vermeeren

Department of Chemistry and Pharmaceutical Sciences, AIMMS, Vrije Universiteit Amsterdam, De Boelelaan 1108, 1081 HZ Amsterdam, The Netherlands.

Email: [p.vermeeren@vu.nl](mailto:p.vermeeren@vu.nl)

### Author Contributions

M.-E. M. initiated and supervised the project. P.M.P.-G. performed the experiments and analyzed the data with the contributions of M.L.G.S.-P. and M.-E. M. DFT calculations and QTAIM analysis was performed by M.L.G.S.-P. EDA analyses were performed by M.L.G.S.-P. and P.V. The computational results were analyzed by M.L.G.S.-P., C.F.G., P.V. and M.-E. M. The manuscript was written through contributions of all authors and all authors have given approval to the final version of the manuscript.

‡ P.M.P.-G. and M.L.G.S.-P. contributed equally.

### Funding Sources

European Research Council (ERC) under the European Union's Horizon 2020 research and innovation program (grant agreement No. 715060).

ENW-XS grant (grant number: OCENW.XS21.4.038) from the Dutch Research Council (NWO).

### Notes

The authors declare no competing financial interest.

### ACKNOWLEDGMENT

The authors thank for financial support the European Research Council (ERC) under the European Union's Horizon 2020 research and innovation program (grant agreement No. 715060). P.M.P.-G. acknowledges funding from an ENW-XS grant (grant number: OCENW.XS21.4.038) from the Dutch Research Council (NWO). C.F.G. and P.V. acknowledge the Netherlands Organization for Scientific Research (NWO). This work made use of the Dutch national e-infrastructure with the support of the SURF Cooperative using grant no. EINF-3520.

### REFERENCES

- [1] Brookhart, M.; Studabaker, W. B. Cyclopropanes from reactions of transition metal carbene complexes with olefins. *Chem. Rev.* **1987**, *87*, 411–432.
- [2] Ying, X.; Qiu, D.; Wang, J. Transition-Metal-Catalyzed Cross-Couplings through Carbene Migratory Insertion. *Chem. Rev.* **2017**, *117*, 13810–13889.
- [3] Ogba, O. M.; Warner, N. C.; O'Leary, D. J.; Grubbs, R. H. Recent advances in ruthenium-based olefin metathesis. *Chem. Soc. Rev.* **2018**, *47*, 4510–4544.
- [4] Belov, D. S.; Tejada, G.; Bukhryakov, K. V. Olefin Metathesis by First-Row Transition Metals. *ChemPlusChem* **2021**, *86*, 924–937.
- [5] Takebazashi, S.; Iron, M. A.; Feller, M.; Rivada-Wheellaghan, O.; Leitun, G.; Diskin-Posner, Y.; Shimon, L. J. W.; Avram, L.; Carmieli, S. G. W.; Cohen-Ofri, I.; Rajashekharayya, A. S.; Shenhar, R.; Eisen, M.; Milstein, D. Iron-catalysed ring-opening metathesis polymerization of olefins and mechanistic studies. *Nature Catalysis* **2022**, *5*, 494–502.
- [6] Grubbs, R. H.; Miyashita, A.; Carbon-Carbon Bond Cleavage Reactions in the Decomposition of Metallacycles. *J. Am. Chem. Soc.* **1978**, *100*, 7418–7420.
- [7] Miyashita, A.; Grubbs, R. H. Reactions of nickel-carbene complexes generated from nickelacycle complexes. *Tetrahedron Letters* **1981**, *22*, 1255–1256.
- [8] Mindiola, D. J.; Hillhouse, G. L. Synthesis, Structure, and Reactions of a Three-Coordinate Nickel-Carbene Complex, {1,2-Bis(ditert-butylphosphino)ethane}Ni=CPh<sub>2</sub>. *J. Am. Chem. Soc.* **2002**, *124*, 9976–9977.
- [9] Iluc, V. M.; Hillhouse, G. L. Three-Coordinate Nickel Carbene Complexes and Their One-Electron Oxidation Products. *J. Am. Chem. Soc.* **2014**, *136*, 6479–6488.
- [10] Prakasham, A. P.; Ghosh, P. Nickel N-heterocyclic carbene complexes and their utility in homogeneous catalysis. *Inorganica Chimica Acta* **2015**, *431*, 61–100.
- [11] Gutsulyak, D. C.; Piers, W. E.; Borau-Garcia, J.; Parvez, M. Activation of Water, Ammonia, and Other Small Molecules by PC<sub>carbene</sub>P Nickel Pincer Complexes. *J. Am. Chem. Soc.* **2013**, *135*, 11776–11779.
- [12] Waterman, R.; Hillhouse, G. L. Group Transfer from Nickel Imido, Phosphinidene, and Carbene Complexes to Ethylene with Formation of Aziridine, Phosphirane, and Cyclopropene Products. *J. Am. Chem. Soc.* **2003**, *125*, 13350–13351.
- [13] Mindiola, M.; Smith, M.; Bercaw, J. Gregory L. Hillhouse: His life, His Art, His Science, and the Rise of “Double Nickel”. *Organometallics*, **2015**, *34*, 4633–4636.
- [14] Sansores-Paredes, M. L. G.; van der Voort, S.; Lutz, M.; Moret, M.-E. Divergent Reactivity of an Isolable Nickelacyclobutane. *Angew. Chem. Int. Ed.* **2021**, *60*, 26518–26522.
- [15] Miyashita, A.; Ohyoshi, M.; Shitara, H.; Nohira, H. Preparation and properties of metallacyclobutanes of nickel and palladium. *Journal of Organometallic Chemistry* **1988**, *338*, 103–111.
- [16] te Velde, G.; Bickelhaupt, F. M.; Baerends, E. J.; Fonseca Guerra, C.; van Gisbergen, S. J. A.; Snijders, J. G.; Ziegler, T. *J. Comput. Chem.* **2001**, *22*, 931–967.
- [17] Gaussian 16, Revision C.01, Frisch, M. J.; Trucks, G. W.; Schlegel, H. B.; Scuseria, G. E.; Robb, M. A.; Cheeseman, J. R.; Scalmani, G.; Barone, V.; Petersson, G. A.; Nakatsuji, H.; Li, X.; Caricato, M.; Marenich, A. V.; Bloino, J.; Janesko, B. G.; Gomperts, R.; Mennucci, B.; Hratchian, H. P.; Ortiz, J. V.; Izmaylov, A. F.; Sonnenberg, J. L.; Williams-Young, D.; Ding, F.; Lipparini, F.; Egidi, F.; Goings, J.; Peng, B.; Petrone, A.; Henderson, T.; Ranasinghe, D.; Zakrzewski, V. G.; Gao, J.; Rega, N.; Zheng, G.; Liang, W.; Hada, M.; Ehara, M.; Toyota, K.; Fukuda, R.; Hasegawa, J.; Ishida, M.; Nakajima, T.; Honda, Y.; Kitao, O.; Nakai, H.; Vreven, T.; Throssell, K.; Montgomery, J. A., Jr.; Peralta, J. E.; Ogliaro, F.; Bearpark, M. J.; Heyd, J. J.; Brothers, E. N.; Kudin, K. N.; Staroverov, V. N.; Keith, T. A.; Kobayashi, R.; Normand, J.; Raghavachari, K.; Rendell, A. P.; Burant, J. C.; Iyengar, S. S.; Tomasi, J.; Cossi, M.; Millam, J. M.; Klene, M.; Adamo, C.; Cammi, R.; Ochterski, J. W.; Martin, R. L.; Morokuma, K.; Farkas, O.; Foresman, J. B.; Fox, D. J. Gaussian, Inc., Wallingford CT, **2016**.
- [18] ADF2022, SCM, Theoretical Chemistry, Vrije Universiteit, Amsterdam, The Netherlands, <http://www.scm.com>.
- [19] Vermeeren, P.; van der Lubbe, S. C. C.; Fonseca Guerra, C.; Bickelhaupt, F. M.; Hamlin, T. A. *Nat. Protoc.* **2020**, *15*, 649–667.
- [20] Vermeeren, P.; Hamlin, T. A.; Bickelhaupt, F. M. *Chem Commun.* **2021**, *57*, 5880.
- [21] Bickelhaupt, F. M.; Baerends, E. J. Kohn-Sham Density Functional Theory: Predicting and Understanding Chemistry. In *Reviews in Computational Chemistry*; Lipkowitz, K. B.; Boyd, D. B., Eds.; Wiley-VCH: New York, **2000**, Vol. *15*, pp 1–86.
- [22] Hamlin, T. A.; Vermeeren, P.; Fonseca Guerra, C.; Bickelhaupt, F. M.; “Energy decomposition analysis in the context of quantitative molecular orbital theory”. *Complementary Bonding Analysis*, edited by Simon Grabowsky, Berlin. Boston: De Gruyter, 2021, pp. 199–212.
- [23] Pérez-García, P.M.; Darù, A.; Scheerder, A.R.; Lutz, M.; Harvey, J.N.; Moret, M.-E.T. Oxidative Addition of Aryl Halides to a Triphosphine Ni(0) Center to Form Pentacoordinate Ni(II) Aryl Species. *Organometallics* **2020**, *39*, 1139–1144.
- [24] March, J. The decarboxylation of organic acid. *J. Chem. Educ.* **1963**, *40*, 212–213.

[25] Liu, M.; Le, N.; Uyeda, C. Nucleophilic Carbenes Derived from Dichloromethane. *Angew. Chem. Int. Ed.* **2023**, *62*, e202308913.  
[26] Bader, R. F. W. *Acc. Chem. Res.* **1985**, *18*, 9-15.  
[27] Frenking, G.; Solà, M.; Vyboishchikov, S. F. Chemical bonding in transition metal carbene complexes. *J. Organomet. Chem.* **2005**, *690*, 6178-6204.  
[28] Lu, T.; Chen, F. Multiwfn: A multifunctional wavefunction analyzer. *J. Comput. Chem.* **2012**, *33*, 580-592.  
[29] Occhipinti, G.; Jensen, V. R. Nature of the Transition Metal-Carbene Bond in Grubbs Olefin Metathesis Catalysts. *Organometallics*, **2011**, *30*, *13*, 3522-3529.

[30] Krapp, A.; Pandey, K. K.; Frenking, G. Transition Metal-Carbon Complexes. A Theoretical Study. *J. Am. Chem. Soc.* **2007**, *129*, *24*, 7596-7610.  
[31] Weidman, J. D.; Estep, M. L.; Schaefer III, H. F. *J. Phys. Chem. A* **2018**, *122*, *32*, 6570-6577.

